

Hydrodynamic description of spectra at high transverse mass in ultrarelativistic heavy ion collisions

T. Peitzmann

University of Münster, D-48149 Münster, Germany

the date of receipt and acceptance should be inserted later

Abstract. Transverse mass spectra of pions and protons measured in central collisions of heavy ions at the SPS and at RHIC are compared to a hydrodynamic parameterization. While the chemical temperature needed at RHIC is significantly higher compared to SPS, the spectra may be described using kinetic freeze-out parameters which are very similar for both beam energies. There is no necessity of much stronger transverse flow at RHIC. The contribution of such hydrodynamic emission at high transverse momenta is investigated in detail. It is shown that hydrodynamics may be relevant up to relatively high transverse momenta. The importance of the velocity profile used in this context is highlighted. Implications for the interpretation of elliptic flow are discussed.

PACS. 25.75.Dw Particle and resonance production

1 Introduction

The description of transverse momentum (or transverse mass) spectra with hydrodynamic models is one of the well established tools in ultrarelativistic heavy-ion physics [1,2,3,4,5,6,7,8]. The applicability of such models is still under discussion, because they require local thermalization, which may not hold for the entire reaction volume. Furthermore, at high transverse momenta hard scattering is expected to provide an important contribution to particle production – the exact momentum region where this would apply is under debate.

Comparisons to experimental data have often been performed using parameterizations of hydrodynamic distributions, which have to use simple assumptions about the freeze-out conditions, e.g. mostly one universal freeze-out temperature is used. While such parameterizations can not replace full hydrodynamic calculations, they can provide a reasonable guideline to the general behavior of particle distributions, especially as systematic studies are more accessible in this case due to the much more modest calculational effort.

In the present paper I will assume the validity of hydrodynamic pictures, but I will not attempt to deliver a full-fledged, realistic hydrodynamic calculation. A parameterization will be used to describe momentum spectra at low and intermediate m_T .¹ Parameters for chemical and kinetic freeze-out will be determined from a simultaneous fit of pion and (anti-)proton spectra. While these parameters may be used to compare to other estimates to check their consistency, this is not the main purpose here. Instead, the intention is to use a not too unrealistic hydrodynamic calculation fitted to low transverse masses to study the extrapolation to high m_T .

This is very important also in the light of recent attempts to measure jet quenching at RHIC via transverse momentum distributions [9]. If the particle emission at low m_T is governed by hydrodynamics, as e.g. the results on elliptic flow [10,11] suggest, then such a hydrodynamic source will inevitably contribute at high m_T also. Such a hydrodynamic contribution would have to be subtracted from the measured particle yields before comparing them to pQCD calculations and obtaining estimates of the amount of suppression of hard scattering.

2 The Model

The calculations presented in this paper are based on a hydrodynamic model by Wiedemann and Heinz [4] which includes transverse flow and resonance decays. The original computer program calculates the direct production of pions and the contributions from the most important resonances having two- or three-body decays including pions (ρ , K_S^0 , K^* , Δ , $\Sigma + \Lambda$, η , ω , η'). The transverse momentum spectra of the directly emitted resonances r are given by:

$$\begin{aligned} \frac{dN_r^{\text{dir}}}{dM_T^2} &= \text{const.} \cdot (2J_r + 1) \\ &\times M_T \int_0^4 d\left(\frac{\xi^2}{2}\right) e^{-\xi^2/2} K_1\left(\frac{M_T}{T} \cosh \eta_t(\xi)\right) \\ &\times I_0\left(\frac{P_T}{T} \sinh \eta_t(\xi)\right), \end{aligned} \quad (1)$$

where $\xi = r/R$ and R is the Gaussian radius of the source. The transverse rapidity of the source element is given as $\eta_t(\xi) = \eta_f \xi^n$, where the default value of the power is $n = 1$. The transverse rapidity parameter η_f controls the amount of transverse flow.

¹ While such calculations can also be used to compare to two-particle-correlations, this will not be the scope of this paper.

This distribution represents the rapidity integrated spectrum, which will be used in this paper, as it is easier to calculate compared to the general rapidity differential spectrum. In comparison to experimentally measured spectra, which are mostly from limited rapidity regions, this may introduce a bias. This bias should however be small, if the rapidity dependence of the spectra is negligible as in a longitudinal scaling expansion (Bjorken) scenario.

The original version of this model uses the following assumptions:

1. The spatial density distribution at freeze-out is chosen as a Gaussian.
2. One universal freeze-out temperature is used which determines both the spectral shape and the ratio of different particle species (i.e. resonances).

In the calculations performed here the model has been modified in the following way:

1. As the spatial distribution a Woods-Saxon shape:

$$\rho_{ws}(\xi) = \rho_0 \cdot \frac{1}{1 + \exp \Delta(\xi - 1)} \quad (2)$$

has been introduced. By varying the parameter Δ the shape can be adjusted. For large values of Δ the shape approaches a box-like distribution. The shape may also be chosen very similar to a Gaussian for comparison. The spatial distributions fix implicitly the shape of the velocity distribution. While this may not be very relevant at low transverse momenta, it has been shown to be important at high p_T [7]. The influence of different distributions has also been investigated in [8].

2. The spectra for a given particle (or resonance) are calculated using the kinetic temperature T_{kin} . Finally the normalization is readjusted to the chemical temperature T_{chem} assuming that dN/dy at midrapidity scales with the temperature as [1]:

$$\frac{dn_{th}}{dy} = \frac{V}{(2\pi)^2} T^3 \left(\frac{m^2}{T^2} + \frac{2m}{T} + 2 \right) \exp \left(-\frac{m}{T} \right). \quad (3)$$

It is commonly believed that chemical freeze-out (determining particle ratios) should occur at higher temperature than kinetic freeze-out (determining the spectral shape), so at least two independent temperatures may be needed.

3. Furthermore the program has been enhanced to simultaneously describe protons and antiprotons in addition to pions. Here the decay contributions from Δ and $\Sigma + \Lambda$ have been taken into account. This of course requires the introduction of another parameter: the baryonic chemical potential μ_B .

To better understand the importance of the different shapes of the source distribution, it is helpful to investigate the resulting velocity distributions:

$$\frac{dN}{d\beta_T} = \frac{2\pi\xi}{\eta_f} \cdot \frac{1}{1 - \beta_T^2} \cdot \rho(\xi), \quad (4)$$

as they directly influence the shape of the momentum distribution, while the spatial distribution is actually not directly relevant. Fig. 1 shows velocity distributions for different shapes at

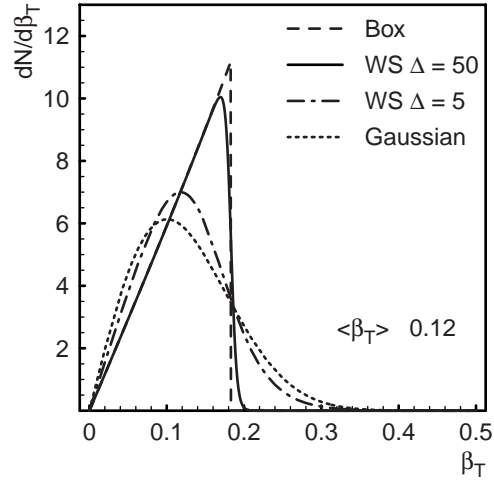


Fig. 1. Velocity distributions of the model source for different source shapes at an average velocity of $\langle\beta_T\rangle = 0.12$.

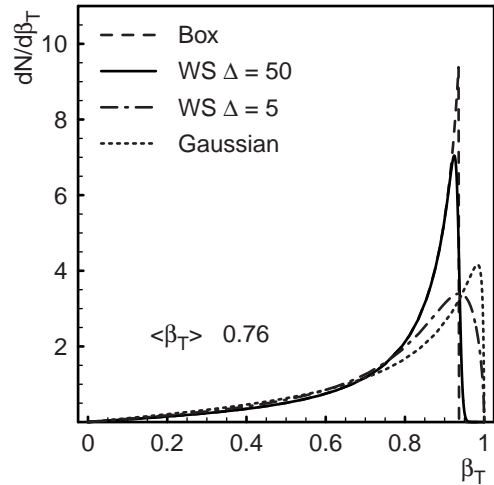


Fig. 2. Velocity distributions as in Fig. 1 at an average velocity of $\langle\beta_T\rangle = 0.76$.

a small average velocity of $\langle\beta_T\rangle = 0.12$. For such small velocities the relation between rapidity and velocity $\beta_T = \tanh \eta_t$ may be approximated by a linear relation, so most of the expected properties of the distributions are preserved. One can see that the box profile yields a sharp cutoff of the velocity distribution. The Woods-Saxon with $\Delta = 50$ looks very similar to the box with a slightly smeared out edge. The Gaussian has a much more smooth edge resulting from the tail of the spatial distribution. The Woods-Saxon with $\Delta = 5$ provides a similar case as the Gaussian, both have considerable contributions at velocities much higher than the average which will finally lead to an enhanced yield at higher transverse momenta for the same inverse slope at a low p_T , i.e. to stronger curvature of the spectrum.

Fig. 2 shows similar distributions for a high average velocity of $\langle\beta_T\rangle = 0.76$. Again the box profile leads to a sharp upper limit in velocity, but the triangular shape of the distribution is distorted from the non-linearity of the relation between β_T and η_t . The Woods-Saxon for $\Delta = 50$ is again similar to the box,

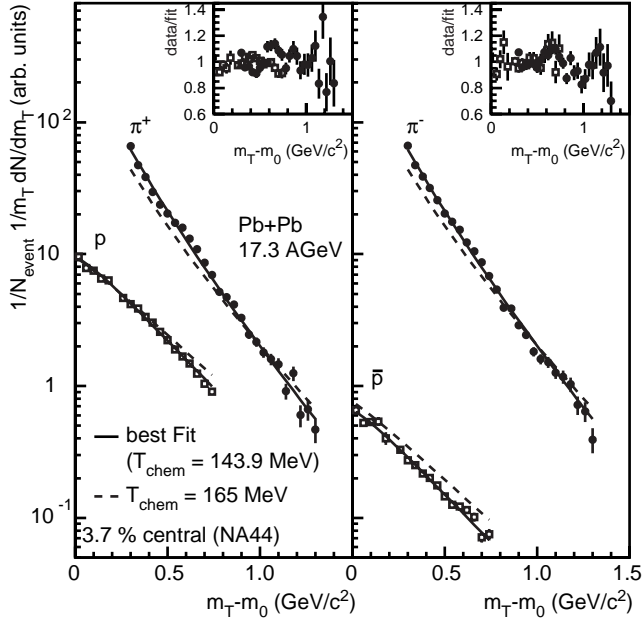


Fig. 3. Transverse mass distributions of pions and (anti-)protons for central Pb+Pb collisions at 158 AGeV from the NA44 experiment [12]. Included are two different fits to the data with the hydrodynamic model discussed in the text.

and the one for $\Delta = 5$ and the Gaussian are also close. However, in this case the two latter distributions have a maximum shifted towards higher velocity which is also due to the non-linearity. Still, the general property of these distributions is that they have larger contributions at high velocities for the same average velocity as the other two distributions.

3 Hadron Spectra from SPS

The model described above has first been compared to data from SPS heavy ion experiments. Data from NA44 on pion, proton and antiproton production in the 3.7 % most central Pb+Pb collisions [12] have been used. The transverse mass spectra are shown in Fig. 3, they cover the range of $0.3 \text{ GeV}/c^2 \leq m_T - m_0 \leq 1.3 \text{ GeV}/c^2$ for pions and $0.02 \text{ GeV}/c^2 \leq m_T - m_0 \leq 0.74 \text{ GeV}/c^2$ for protons and antiprotons. Our model has been fitted to the data. The best agreement can be achieved with a kinetic temperature $T_{kin} = 122.2 \text{ MeV}$, an average transverse flow velocity $\langle \beta_T \rangle = 0.478$, a chemical temperature $T_{chem} = 143.9 \text{ MeV}$ and a baryonic chemical potential $\mu_B = 193.3 \text{ MeV}$. For this fit the width parameter has been set to $\Delta \equiv 50$, allowing for a free variation of this parameter produces a slightly smaller value with a very large error while the other parameters remain unchanged. As the fits seem to be insensitive to small changes in Δ , we have performed most fits with a fixed value. For systematic checks some of the constraints on the fits have been varied. Most of these changes, as e.g. omitting some of the data points (the lowest or highest in m_T , resp.) from the fit, do not affect the parameter values significantly. Significant changes are obtained under the following conditions:

1. All contributions from weakly decaying particles are ignored. In this case the chemical temperature and the baryonic chemical potential change slightly, while the kinetic temperature and the flow velocity are essentially unaltered. This is understandable as the particle ratios may depend more strongly on this contribution than the shape of the spectra. As the quality of the fit is similar to the best fit above and a not precisely specified fraction of weak decays may contribute to the data, this has to be taken into account in the systematic error.
2. The width parameter is set to $\Delta \equiv 5$. In this case the chemical parameters show small changes, while the temperature and flow velocity change more significantly. This is mainly due to the fact that this spatial distribution, which is similar to a Gaussian, results in a broader velocity distribution. The quality of the fit is significantly worse than the fits given above.
3. The kinetic and chemical temperatures have been set to the same value of $T \equiv 144 \text{ MeV}$ and the chemical potential to $\mu_B = 193.3 \text{ MeV}$.

Here, the flow velocity obtained is smaller than in the best fit, as is expected for a higher kinetic temperature. Again the fit quality is worse.

4. The expansion velocity has been fixed to a value of $\langle \beta_T \rangle = 0.55$. The fit quality is much worse than the best fit.
5. The chemical temperature has been set to $T_{chem} \equiv 165 \text{ MeV}$ similar to results from fits of hadrochemical models to ratios of total multiplicities of different species [13].

This fit cannot describe the spectra, it essentially has the wrong ratio of pions to protons. Of importance may be the different integration region in rapidity compared to [13]. If e.g. the rapidity distribution of protons is broader than the one of pions this may easily explain the smaller chemical temperature obtained here. However, for the purpose of this paper, we will just note this discrepancy and use the fit results as they are. The parameters obtained apparently describe the particle ratios at midrapidity investigated here, and this may be the relevant information which should be used also in estimating the contribution of resonances to the momentum spectra at this given rapidity.

Furthermore, it may be that part of the longitudinal motion of the source is not generated hydrodynamically but is a remnant of the initial state motion, which may be even more likely for participant protons. In this case it is not completely obvious, whether the protons observed at very different rapidities share the same chemical freeze-out temperature. If the spacetime-momentum correlation originates from a very early phase of the collision, a unique chemical temperature might not be applicable and the use of integrated multiplicities might be misleading. Rather, there is the possibility of a local temperature which may be applicable for limited rapidity regions.

The fit parameters obtained from the fits discussed above are summarized in table 1. None of the fits provides a perfect agreement with the data, which is due to a structure in the experimental spectra which can not be described within this model.

While the data used above have a limited range in transverse mass, one might also consider comparing such hydrody-

Table 1. Fit parameters of hydrodynamic fits to pion and (anti-)proton spectra in central Pb+Pb collisions at the CERN SPS. The errors given are statistical. An error of 0 indicates that this parameter was fixed in the fit.

Remarks	χ^2/ν	T_{kin} (MeV)	η_f	$\langle\beta_T\rangle$	T_{chem} (MeV)	μ_B (MeV)	Δ
best fit	217/82	122.2 ± 1.9	0.805 ± 0.007	0.478 ± 0.004	143.9 ± 0.6	193.3 ± 0.9	50 ± 0
no weak decays	217/82	120.4 ± 1.9	0.804 ± 0.007	0.478 ± 0.004	150.9 ± 0.4	202.6 ± 0.9	50 ± 0
modified width	360/82	95.6 ± 3.0	0.745 ± 0.010	0.517 ± 0.007	146.3 ± 0.4	196.4 ± 0.9	5 ± 0
$T_{kin} = T_{chem}$	358/85	144 ± 0	0.728 ± 0.004	0.442 ± 0.002	144 ± 0	193.3 ± 0	50 ± 0
high $\langle\beta_T\rangle$	799/83	92.7 ± 0.9	0.968 ± 0	0.55 ± 0	144.6 ± 0.4	193.2 ± 0.9	50 ± 0
high T_{chem}	2394/83	156.3 ± 3.0	0.802 ± 0.001	0.477 ± 0.001	165 ± 0	208.4 ± 0.8	50 ± 0

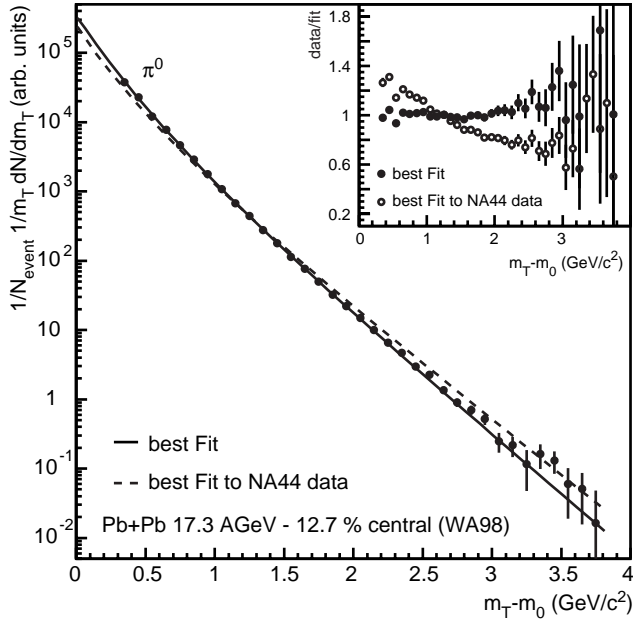


Fig. 4. Transverse mass distributions of neutral pions for the 12.7% most central Pb+Pb collisions at 158 AGeV from the WA98 experiment [14]. Included are two different fits to the data with the hydrodynamic model discussed in the text.

dynamic distributions to data with a wider transverse momentum range. This has actually been done before at the SPS by WA98 [7], using also a program derived from the one of Wiedemann and Heinz [4]. However in this version the original assumption of the same temperature both for chemical and kinetic freeze-out was applied. Also, only neutral pion spectra were used, which give very limited information to determine all relevant parameters.

In the following, information from the fits to NA44 data above will be used while fitting the neutral pion spectra of WA98 [14]. Ideally one might just try to use exactly the same fit and compare it to the neutral pions. As the data are from different experiments and do not exactly use the same centrality selections, the normalization has to be kept as a free parameter. The centrality selections used below should however be similar enough, so that the shape of the spectra should not differ strongly.

In Figure 4 fits using the parameters obtained above (“best fit” in table 1) are compared to the neutral pion spectra for the 12.7% most central reactions of Pb+Pb at 158 AGeV. The fit is shown as a dashed line. The description is only superficially

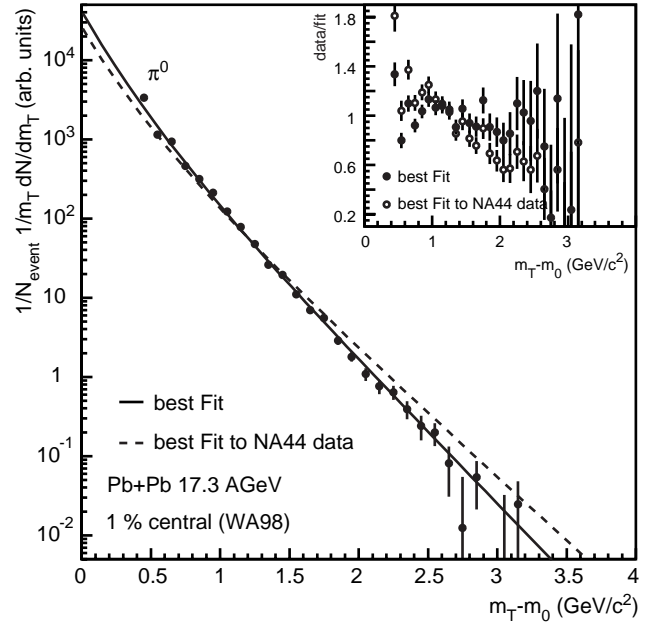


Fig. 5. Transverse mass distributions of neutral pions as in Figure 4 for the 1% most central Pb+Pb collisions at 158 AGeV from the WA98 experiment [14].

adequate, the fit overshoots the data at large transverse masses, and one obtains a $\chi^2/\nu = 712/20$. Another fit has been performed keeping only the parameters T_{chem} and μ_B the same as in the earlier fit and optimizing the kinetic temperature and the flow for the neutral pions. This fit (shown as a solid line) yields a good description with $\chi^2/\nu = 27/18$. The fit parameters obtained are $T_{kin} = 130.3$ MeV and $\langle\beta_T\rangle = 0.415$. The (dis-)agreement of the fits can also be judged from the inset in Figure 4, which shows the ratios of the data to the fits.

One might argue that the different centrality selections are responsible for the disagreement. Although this does not seem to be very likely, as it has been shown [14], that the shape of the pion spectra does not vary strongly for medium-central to central collisions, a comparison to the 1% most central data has been performed. The results are displayed in Figure 5. Again the dashed line shows a fit with all parameters fixed as above ($\chi^2/\nu = 114/14$), which also overshoots the data at high m_T . The solid line shows a relatively good fit ($\chi^2/\nu = 32/12$) with $T_{kin} = 113.0$ MeV and $\langle\beta_T\rangle = 0.763$. The different parameters for this second fit compared to the other central (12.7%) sample are most likely not conclusive, but are an example that fitting momentum spectra of just one particle species leaves an

ambiguity in the parameters. The higher flow velocity can be compensated by a lower temperature and vice versa. Also I will not put too much emphasis on the fact that the fits to the NA44 data appear to overpredict the pion yield at high p_T , because part of this discrepancy might be due to systematic differences between the two experiments involved.

One can however note that already under conservative assumptions this hydro model can account for essential all of the pion production at high p_T . Here a profile with a negligible tail towards higher velocities ($\Delta = 50$ – similar to the box profile) has been used. A more diffuse profile ($\Delta = 5$) would necessarily lead to a larger discrepancy at high p_T . Most of the other systematic variations studied do not lead to significant variations in this respect. A fixed chemical temperature of $T_{chem} \equiv 165$ MeV leads to different results, but from Fig. 3 it is obvious that this would also lead to a larger overprediction at high p_T . As sketched above, there may be reasons why this assumption may not be adequate for our analysis. In fact, it has been remarked in [15,16] that there is a rapidity dependence of chemical parameters. The chemical temperature of $T_{chem} = 143.9$ MeV and the baryo-chemical potential of $\mu_B = 193.3$ MeV of the best fit can be compared to results of other analyses. As stated above, the temperature is lower than the values of $T_{chem} = 158 \pm 3$ MeV [17] and $T_{chem} = 168 \pm 2.4$ MeV [13] obtained from rapidity integrated yields, but compares well with the result $T_{chem} = 141 \pm 5$ MeV given in [12].

4 Hadron Spectra from RHIC

The situation at RHIC is more favorable for this analysis, as there exist data on different particle species partially reaching out to large p_T measured under the same conditions within one experiment. The PHENIX experiment has presented spectra of neutral pions [9] and identified charged hadrons [18,19] in central Au+Au collisions at $\sqrt{s_{NN}} = 130$ GeV. A similar procedure as for the SPS data above is followed. Fits are performed to the charged pions for $m_T - m_0 < 2$ GeV/c and to (anti)protons for $m_T - m_0 < 3$ GeV/c. Systematic variations of the fitting assumptions are done as above. In addition we have studied fits to a limited transverse mass range $m_T - m_0 < 1.5$ GeV/c for pions and (anti)protons. The results are summarized in table 2, a comparison of the fits to the data is shown in Fig. 6.

The best fit in this case is obtained using a profile with $\Delta = 5$, i.e. more Gaussian-like (fit A in table 2). A chemical temperature $T_{chem} = 171.5$ MeV and a baryo-chemical potential of $\mu_B = 36.8$ MeV are obtained, which are very similar to the results in [21] where $T_{chem} = 174 \pm 7$ MeV and $\mu_B = 46 \pm 5$ MeV are given. The better agreement at RHIC compared to SPS of the chemical parameters of this analysis with those of the integrated yields may be related to the fact that boost invariance is a much better approximation in the RHIC case. The kinetic temperature is determined to $T_{kin} = 122.7$ MeV with an average transverse flow velocity $\langle \beta_T \rangle = 0.445$.

A fit with a different profile ($\Delta = 50$) yields similar parameters but is significantly worse in χ^2 (fit B in table 2). A fit assuming a unique temperature of $T = 165$ MeV for both

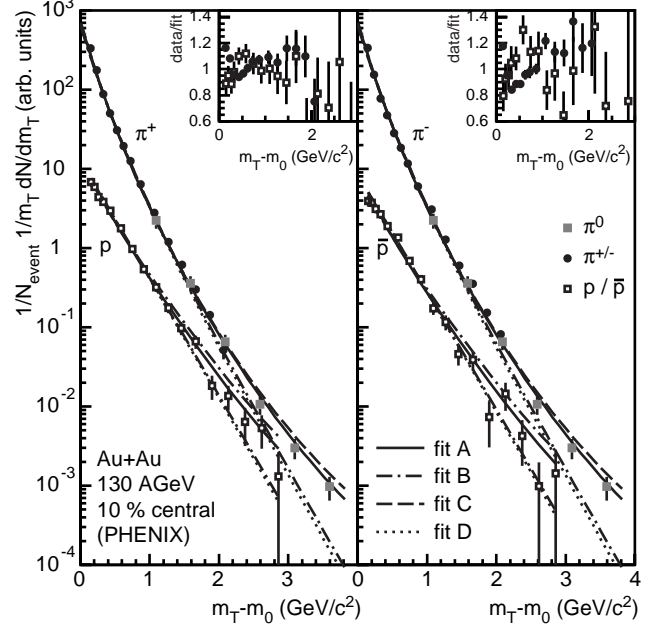


Fig. 6. Transverse mass distributions of pions and (anti)protons for the 10% most central Au+Au collisions at $\sqrt{s_{NN}} = 130$ GeV from the PHENIX experiment [9,18,19].

kinetic and chemical freeze-out as in [20] is again much worse in fit quality, in fact it yields the largest χ^2 of all fits investigated. As the assumption of simultaneous kinetic and chemical freeze-out underlying this fit is questionable, it will not be considered further. A fit ignoring weak decays does not yield very significant differences in line with the analog analysis of SPS data. One might argue that the transverse mass range used in these fits does include possible contributions of hard scattering. However, fits which use data only for $m_T - m_0 < 1.5$ GeV/c yield very similar results (fits C and D in table 2).

From the comparison of fits A-D in Fig. 6 the biggest systematic uncertainty in the different fits is easily seen. In the figure also the neutral pion data of PHENIX [9] are included, which are not used in the fits. While all fits are relatively similar at low $m_T - m_0$ there is a difference at high transverse mass. While the fits with a box-like profile ($\Delta = 50$) strongly underpredict the neutral pions, the Gaussian-like fits ($\Delta = 5$) can describe the pion spectra completely. There is a similar difference in the protons, but the errors of the experimental data do not allow a strong statement there.

5 Discussion

The results for SPS and RHIC data may now be compared to each other and to other calculations. The best fits in both cases yield kinetic freeze-out temperatures of $T_{kin} \approx 120$ MeV and average flow velocities of $\langle \beta_T \rangle \approx 0.45$. In fact, the RHIC data indicate even a slightly smaller expansion velocity, which is of course related to the different velocity profiles used for the two cases. With these two fits it is possible to describe the pion and (anti-)proton spectra over the full momentum range in the two cases. Using the same (box-like) profile in both cases, sim-

Table 2. Fit parameters of hydrodynamic fits to pion and (anti-)proton spectra in central Au+Au collisions at RHIC. The errors given are statistical. An error of 0 indicates that this parameter was fixed in the fit.

Remarks	χ^2/ν	T_{kin} (MeV)	η_f	$\langle\beta_T\rangle$	T_{chem} (MeV)	μ_B (MeV)	Δ
best fit (A)	287/57	122.7 ± 5.4	0.612 ± 0.018	0.445 ± 0.013	171.5 ± 1.7	36.8 ± 3.7	5 ± 0
no weak decays	332/57	113.6 ± 6.0	0.634 ± 0.020	0.393 ± 0.012	181.8 ± 2.3	39.8 ± 4.0	5 ± 0
modified width (B)	368/57	136.7 ± 5.8	0.742 ± 0.028	0.448 ± 0.017	173.8 ± 1.7	34.2 ± 3.7	50 ± 0
$T_{kin} = T_{chem}$	449/59	165 ± 0	0.459 ± 0.050	0.351 ± 0.038	165 ± 0	41 ± 0	5 ± 0
low m_T only (C)	242/39	105.3 ± 6.5	0.677 ± 0.023	0.481 ± 0.016	170.5 ± 1.8	35.6 ± 3.8	5 ± 0
low m_T only (D)	326/39	131.3 ± 6.3	0.754 ± 0.031	0.454 ± 0.019	172.9 ± 1.7	33.8 ± 3.7	50 ± 0

ilar velocities are obtained, but the freeze-out temperature is slightly higher at RHIC. This finding is in contradiction with the result presented in [22] that the collective flow is stronger at RHIC. It can, however, be seen in [22] that this is strongly influenced by the proton and antiproton spectra from STAR used in the analysis, which show a much larger inverse slope than the PHENIX results.

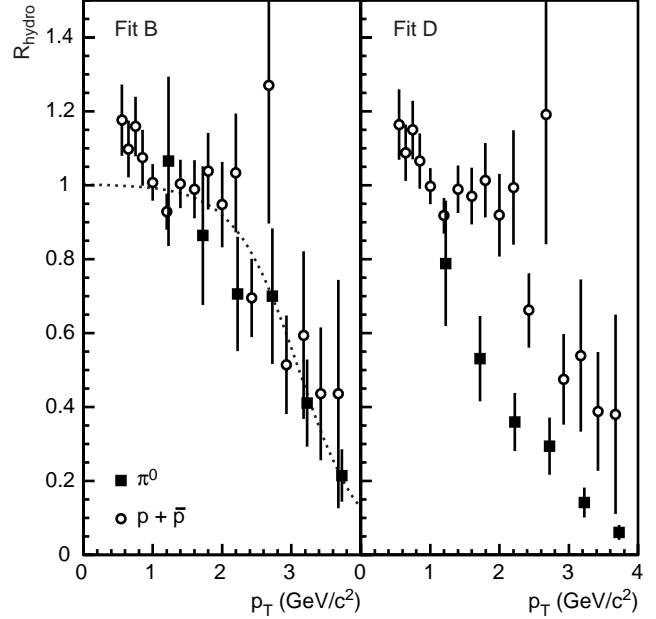
From the SPS data it is clear that a Gaussian-like profile, which leads to an overprediction of the pion yield at high m_T , is excluded. It was already discussed in [7] that a box-like profile would be required in case of a large flow velocity, and this was also found to be the preferred profile in [8]. Assuming a very large flow velocity of $\langle\beta_T\rangle \approx 0.55$ as in [5] and [8], a temperature of $T_{kin} \approx 90$ MeV would be required, in line with the results of [8], but contradicting the values quoted in [5], however, no good fit can be obtained. The present results for the best fit appear to agree with the values given in [22], which are also derived from SPS data.

In any case, no matter what the precise values of the freeze-out parameters are, if particle production at low m_T in heavy-ion collisions at the SPS is ascribed to hydrodynamic scenarios, the extrapolation of the hydrodynamic contribution to high m_T will leave very little room for additional production mechanisms, e.g. hard scattering. It is perceivable that even at low m_T there are contributions to particle production other than hydrodynamic, which would be important enough to alter the momentum distributions significantly. Then no strong statement could be made on the yield at high m_T , however, this would also imply that none of the hydrodynamic descriptions of spectra could provide information about the properties of the system.

At RHIC we are facing two extreme scenarios in this context:

1. The velocity profile at freeze-out is different compared to SPS. While the freeze-out temperature and average velocity are similar to the SPS case, the profile leads to more important contributions at high transverse mass. The transverse mass distributions of both pions and (anti-)protons can be explained entirely by such a hydrodynamic source.
2. The velocity profiles for SPS and RHIC are both box-like. The average velocity at RHIC is similar to the SPS, while the kinetic freeze-out temperature is slightly larger. Additional production mechanisms are needed at high m_T , but the hydrodynamic contribution is not negligible.

In case 1 as for the SPS there would be no room for hard scattering production. Case 2 may be considered more conservative, as the assumptions are similar for SPS and RHIC, so we

**Fig. 7.** Fraction of the hydrodynamic component of the neutral pion and proton+antiproton yield using fits B and D from table 2. The dotted line in the left hand figure shows a fit of a Woods-Saxon function to the data (see text).

will have a closer look at fits B and D, which both use these assumptions. In Fig. 7 ratios of the fits to the experimental data, i.e. the fractions R_{hydro} of the produced particles accounted for by the hydrodynamic model, are shown for neutral pions (solid squares) and for protons+antiprotons (open circles) as a function of p_T . On the left hand side the fits to larger m_T ranges and on the right hand side those to the low m_T range only are used.

The proton+antiproton yield is sufficiently described up to $p_T \approx 2.5$ GeV/c, even above $p_T = 3$ GeV/c more than 40% of the yield is due to hydrodynamic production in both fits. The hydrodynamic contribution to pions changes slightly for the different fits. While here hydrodynamics dominates also at lower p_T , there is a steady decrease of the contribution towards higher p_T . But even for the most conservative fit (D), the hydrodynamic contribution to the pion yield for $2 \text{ GeV}/c \leq p_T \leq 3 \text{ GeV}/c$ is about 30 – 40%.

The estimates of the fraction of hydrodynamic production can be used for further comparisons to other experimental data. As an example I will use the estimate following fit (B) to compare to elliptic flow at RHIC. For this purpose the results shown

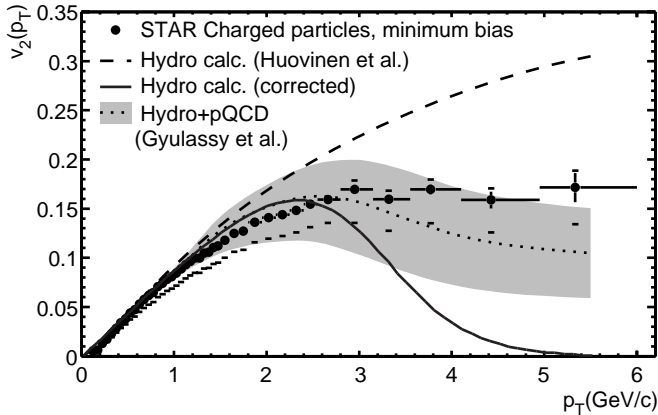


Fig. 8. Strength v_2 of the elliptic flow of charged particles in Au+Au collisions at $\sqrt{s_{NN}} = 130$ GeV as measured by the STAR experiment [23]. The dashed curve shows hydrodynamic calculations from [24] and the dotted line with the grey band estimates from hydrodynamics including jet quenching [25]. The solid line shows an estimate of a fractional hydrodynamic contribution (see text).

in Fig. 7 on the left are fitted with a Woods-Saxon function as displayed in the figure by a dotted line. This will be used in a comparison to results on v_2 for charged particles [23]. Fig. 8 shows the values from STAR for minimum bias Au+Au collisions. As a dashed line the results from hydrodynamic calculations [24] are shown. As discussed in [23] the experimental values follow the hydrodynamic prediction for small transverse momenta. For $p_T > 2$ GeV/c the data level off and deviate from the hydrodynamic curve which continues to rise. This deviation occurs at a similar p_T as the deviation of the hydrodynamic fits from the single particle spectra.

If a certain fraction of particles does not take part in the hydrodynamic evolution in later stages, as represented by p_T spectra, it is unlikely that it should carry hydrodynamic information from the earlier phase, where elliptic flow is generated. It is therefore reasonable to assume that only a similar fraction of the hydrodynamic limit of v_2 should be measurable. The values of v_2 from [24] have therefore been multiplied by the fraction R_{hydro} obtained above, the result is shown as a solid line in Fig. 8. This modified calculation shows indeed a slightly better description up to almost $p_T = 3$ GeV/c, however the estimate of v_2 is much too low at still higher p_T , where the data show a saturation. This comparison calls for another mechanism for producing an elliptic asymmetry at high p_T . Jet quenching has been discussed as such a mechanism [26,25] and calculations of these effects [25] have been included in Fig. 8 as a dotted line. (The grey band shows the variation of the calculations for different densities as discussed in [25].)

The conclusions drawn depend crucially on the type of fit used for the singles spectra. If the more diffuse velocity profile is used, which results in a better description of the spectra with significant deviations of R_{hydro} from one only above $p_T = 3$ GeV/c, the simple prescription applied above would yield an overprediction of v_2 from the hydrodynamic component alone. One should however note, that while the hydrodynamic fraction seen in the spectra might possibly serve as an upper limit estimate for the same fraction relevant for elliptic

flow, the reverse is not necessarily true. A satisfactory treatment would require a detailed hydrodynamic calculation of both effects which is beyond the scope of this paper.

The comparison presented here should serve as illustration that a simultaneous calculation of effects of hydrodynamics and of particle production and quenching in pQCD on both singles spectra and elliptic flow is desirable, as these two observables will be differently influenced by quenching effects. Important hydrodynamic contributions in spectra at high p_T require even stronger quenching of hard scattering production. In return, quenching is a necessary condition to achieve locally equilibrated distributions. In elliptic flow measurements at high p_T the asymmetry may be explained both by hydrodynamics and by partial quenching, the relative importance of each of the mechanisms being still unclear.

6 Summary

Results of hydrodynamic fits to momentum spectra at mid-rapidity in heavy ion reactions at the SPS and at RHIC have been presented. At SPS a chemical temperature of $T_{chem} \approx 145$ MeV and a baryo-chemical potential of $\mu_B \approx 200$ MeV have been obtained, while at RHIC the corresponding values are $T_{chem} \approx 170$ MeV and $\mu_B \approx 35$ MeV. The kinetic parameters are $T_{kin} \approx 120$ MeV and $\langle\beta_T\rangle \approx 0.48$ at SPS and $T_{kin} \approx 135$ MeV and $\langle\beta_T\rangle \approx 0.45$ at RHIC when using a velocity profile similar to a box profile. The analysis does not indicate a significantly stronger transverse flow at RHIC. The momentum spectra of protons can be nicely described in both cases. While at the SPS the momentum spectra of pions may be completely described by these fits, the pion spectra at RHIC leave room for additional particle production mechanisms at high p_T . Estimates of the suppression of hard scattering should, however, take the non-negligible contribution from a hydrodynamic source into account. Studies of elliptic flow should be confronted with simultaneous descriptions of momentum spectra.

The author would like to thank U.A. Wiedemann for helpful discussions and M. Kaneta for valuable information regarding the NA44 data.

References

1. E. Schnedermann, J. Sollfrank, and U. Heinz, Phys. Rev. C **48** (1993) 2462.
2. S. Chapman, J. R. Nix and U. Heinz, Phys. Rev. C **52** (1995) 2694.
3. P. Braun-Munzinger et al., Phys. Lett. B **344** (1995) 43.
4. U.A. Wiedemann and U. Heinz, Phys. Rev. C **56** (1997) 3265.
5. NA49 Collaboration, H. Appelshäuser et al., Eur. Phys. J. C **2** (1998) 661–670.
6. WA80 Collaboration, R. Albrecht et al., Eur. Phys. J. C **5** (1998) 255.
7. WA98 Collaboration, M.M. Aggarwal et al., Phys. Rev. Lett **83** (1999) 926.
8. B. Tomasik, U.A. Wiedemann, and U. Heinz, preprint nucl-th/9907096.

9. PHENIX Collaboration, K. Adcox et al., Phys. Rev. Lett. **88** (2002) 022301.
10. STAR Collaboration, C. Adler et al., Phys. Rev. Lett. **87** (2001) 182301.
11. PHENIX Collaboration, K. Adcox et al., submitted to Phys. Rev. Lett., preprint nucl-ex/0204005.
12. NA44 Collaboration, I.G. Bearden et al., submitted to Phys. Rev. C, preprint nucl-ex/0202019.
13. P. Braun-Munzinger, I. Heppe, and J. Stachel, Phys.Lett. B **465** (1999) 15-20.
14. WA98 Collaboration, M.M. Aggarwal et al., Eur. Phys. J. C **23** (2002) 225-236.
15. J. Sollfrank, U. Heinz, H. Sorge, and N. Xu, Phys. Rev. C **59** (1999) 1637.
16. M. Kaneta, and N. Xu, J. Phys. G **27** (2001) 589.
17. F. Becattini, J. Cleymans, A. Keränen, E. Suhonen, and K. Redlich, Phys. Rev. C **64** (2001) 024901.
18. PHENIX Collaboration, K. Adcox et al., Phys. Rev. Lett. **88** (2002) 242301.
19. PHENIX Collaboration, J. Velkovska et al., talk at ICPA-QGP 2001 Jaipur, to be published in Pramana - Journal of Physics.
20. W. Broniowski and W. Florkowski, Phys.Rev.Lett. **87** (2001) 272302.
21. P. Braun-Munzinger, D. Magestro, K. Redlich and J. Stachel, Phys. Lett. B **518** (2001) 41-46.
22. N. Xu and M. Kaneta, Nucl. Phys. A **698** (2002) 306c.
23. STAR Collaboration, C. Adler et al., submitted to Phys. Rev. Lett, preprint nucl-ex/0206006.
24. P. Huovinen, P.F. Kolb, U.W. Heinz, P.V. Ruuskanen, and S.A. Voloshin, Phys. Lett. B **503** (2001) 58.
25. M. Gyulassy, I. Vitev, and X.N. Wang, Phys. Rev. Lett. **86** (2001) 2537.
26. X.N. Wang, Phys. Rev. C **86** (2001) 054902.